Mon. Not. R. astr. Soc. (1986) **219,** 357–372

Oscillatory motions in intense flux tubes

S. S. Hasan★ *Department of Theoretical Physics, University of Oxford, 1 Keble Road, Oxford OX1 3NP*

Accepted 1985 October 7. Received 1985 September 12; in original form 1985 August 6

Summary. The detailed nature of oscillatory motions in intense flux tubes is examined. We consider states of constant β (the ratio of gas to magnetic pressure) and analyse the character of motions that can occur in such tubes. We include heat exchange between the tube and the ambient medium using Newton's law of cooling. Adopting a linear analysis, we present results for both polytropic and real atmospheres. In the latter case, we use a height dependent radiation exchange time constant. For purposes of comparison with earlier studies, results for the adiabatic case are also given. Growth rates, oscillation frequencies and eigenvectors of the fundamental modes are calculated for different values of the initial magnetic field strength, parametrized by β, and initial tube radius. The latter quantity influences heat exchange, particularly in the optically thick layers. It is found that for the solar stratification, oscillatory behaviour occurs for $\beta<\beta_c$, where β_c denotes some critical value, which depends upon the radius of the tube. Moreover, in the solar case the oscillations are overstable with periods and growth rates typically in the ranges 650–1500 s and 625–1150 s respectively. An interesting feature of the solutions is the existence of a bifurcation at $\beta=\beta_c$ from overstability into two purely unstable modes. Results depicting the height dependence of the eigenvectors (in general complex) and their phases are presented as well. We also examine the sensitivity of the results on boundary conditions. Lastly, some of the observational consequences of the study are pointed out.

1 Introduction

The existence of intense flux tubes with kG field strengths as a dominant feature of the solar atmosphere has been reasonably well established by observations. Theoretically, there has been some debate on the exact nature of the process that produces the kG field. Recently, much interest has focused on the suggestion by Parker (1978) that the principal cause might be a convective instability. This instability has been fairly extensively studied, both in the linear regime (e.g. Webb & Roberts 1978; Spruit & Zweibel 1979) as well as in the non-linear regime (e.g. Hasan 1984a, b; Nordlund 1983). In Hasan (1984a) the non-linear development of the

★Permanent address: Indian Institute of Astrophysics, Bangalore 560034, India.

instability for the solar stratification was examined assuming adiabatic conditions. It was found that the end state that developed was one with stationary oscillations and in which the average value of the magnetic field at the surface was in the kG range. This analysis was generalized in Hasan (1984b) to incude radiative heat exchange between the flux tube and the surrounding medium. Inclusion of heat exchange led to the generation of overstable oscillations (in time) along the magnetic field. Their existence had been conjectured earlier on qualitative grounds by Spruit (1979a).

The main aim of the present study is to examine in detail the nature of motions that can arise in intense flux tubes. A similar problem was investigated in connection with sunspots by Syrovatskii & Zhugzhda (1968), who showed that for a polytropic atmosphere, overstability could occur under certain conditions.* For large values of the polytropic index, their instability criterion turned out to be less severe than the usual Schwarzschild condition for convection in a field-free medium. In the case of intense flux tubes, which can effectively be regarded as 'thin', the problem in the adiabatic approximation, was investigated amongst others by Roberts & Webb (1978); Webb & Roberts (1978) and Spruit & Zweibel (1979) (see also Spruit 1979a, 1982). The more general case of heat exchange based on Newton's law of cooling was incorporated subsequently by Webb & Roberts (1980). Their analysis assumed an isothermal atmosphere and is, therefore, of rather limited applicability (roughly on length scales which are smaller than the local pressure scale height). We shall relax this constraint in favour of a realistic temperature stratification. We shall also treat the polytropic case which is amenable to an analytic solution. For mathematical reasons, we shall work within the framework of the thin flux tube approximation.

There are a variety of wave modes that can exist in thin flux tubes (Spruit 1982). We shall solely concern ourselves with the axisymmetric mode (or 'sausage mode'), which is a longitudinal compressive mode. Physically, it can be regarded as a slow magneto-acoustic oscillation which travels along field lines with a speed given by the expression

$$c_t = \frac{c_s c_a}{\sqrt{c_s^2 + c_a^2}}$$

where c_s and c_a are the sound speed and Alfvén speed respectively in the medium. Owing to radiative coupling between the flux tube and the external gas, these waves can either be damped or become overstable depending upon thermodynamic conditions as we shall see later on. It is, thus, of some interest to quantitatively examine for a sufficiently general range of parameters the conditions under which we have overstability, instability and damped oscillations. We do this by solving the generalized eigenvalue problem, thereby determining the eigenfrequencies (in general complex) of the tube. We also calculate eigenvectors and phase relations between different variables. The sensitivity of the results on boundary conditions is also considered.

The plan of the paper is as follows: in Section 2, we present the thin flux tube equations which can be combined to yield a single second order differential equation for the velocity amplitude. Its solutions for both polytropic and real stratifications are presented in Sections 3 and 4. In the former case an analytic solution is possible whereas in the latter case a numerical solution is attempted using model opacities. The results are described in Section 5 and discussed in Section 6. Finally, some of their observational implications are pointed out in Section 7 followed by concluding remarks.

2 Equations

We adopt the thin flux tube approximation, and consider the MHD equations for a vertical flux tube to zeroth order in a cylindrical coordinate system (r, θ, z), assuming no θ dependence, i.e. we restrict ourselves to the axisymmetric mode.

*This was also found by Roberts (1976) for a Boussinesq fluid.

For the initial unperturbed state we assume hydrostatic equilibrium and equal temperatures in the flux tube and the external medium at each height. Thus, in the initial state, we have

$$\frac{dp_0}{dz} = -\varrho_0 g \tag{1}$$

$$T_0 = T_e \tag{2}$$

$$p + \frac{B_0^2}{8\pi} = p_e \tag{3}$$

where p, T_0 and B_0 denote the pressure, temperature and magnetic field in the unperturbed state and e denotes quantities in the external medium. Equation (3) expresses horizontal pressure balance between the flux tube and its surroundings. Defining $\beta = 8\pi p_0/B^2$, it is easy to see that β is constant with z (strictly speaking only approximately constant as $\mu_0 \approx \mu_e$, where μ is the mean molecular weight). The radius of the flux tube is found from the flux conservation condition

$$B_0 a_0^2 = \text{constant}. \tag{4}$$

Let us now consider small perturbations about this initial state. The linearized MHD equations for the perturbed quantities are (Roberts & Webb 1978):

$$B_0\left\{\frac{\partial \varrho}{\partial t} + \frac{\partial}{\partial z}(\varrho_0 v)\right\} - \varrho_0\left\{\frac{\partial B}{\partial t} + v\frac{dB_0}{dz}\right\} = 0 \tag{5}$$

$$\varrho_0 \frac{\partial v}{\partial t} = -\varrho g - \frac{\partial p}{\partial z} \tag{6}$$

$$\frac{\partial p}{\partial t} + v\frac{dp_0}{dz} = \frac{\gamma p_0}{\varrho_0}\left(\frac{\partial \varrho}{\partial t} + v\frac{d\varrho_0}{dz}\right) + \frac{p_0 \chi_T}{C_v}\dot{Q}_{rad} \tag{7}$$

$$p + \frac{B_0 B}{4\pi} = 0 \tag{8}$$

where ϱ is the density, v the vertical velocity, T the temperature, $\dot{Q}_{rad}$ is the amount of energy per unit mass per unit time exchanged with the ambient medium due to radiative transport, C_v is the specific heat at constant volume, χ_T and χ_ϱ are defined as follows:

$$\chi_T \equiv \left(\frac{\partial \ln p}{\partial \ln T}\right)_\varrho = 1 - \left(\frac{\partial \ln \mu}{\partial \ln T}\right)_\varrho,$$

$$\chi_\varrho \equiv \left(\frac{\partial \ln p}{\partial \ln \varrho}\right)_T = 1 - \left(\frac{\partial \ln \mu}{\partial \ln \varrho}\right)_T,$$

where $\gamma = \chi_\varrho C_p/C_v$. We neglect any time variations in quantities associated with the external medium, i.e. p_e is constant. Equation (6) is a generalized energy equation which includes radiative exchange and also the effect of changes in ionization. We assume that radiative exchange occurs through Newton's law of cooling and set

$$\dot{Q}_{rad} = C_v\left(\frac{T_e - T}{\tau_r}\right), \tag{8}$$

where the time constant τ_r is, following Spiegel (1957), given by

$$\tau_r=\frac{C_v}{16\varkappa\sigma T^3}\{1-\operatorname{arcot}(\varkappa\varrho_0 a_0)\}^{-1}, \tag{9}$$

which in the optically thin ($\varkappa\varrho_0 a_0\ll 1$) and thick ($\varkappa\varrho_0 a_0\gg 1$) limits reduces to $C_v/16\varkappa\sigma T^3$ and $3\varkappa\varrho^2 a^2 C_v/16\varkappa\sigma T^3$ respectively. (We have replaced the wave number in the original expression by a_0, the radius of the flux tube.) In equation (9), $\varkappa$ denotes the opacity and σ is the Stefan–Boltzmann constant.

Assuming that all perturbed quantities have a time dependence of the form $\exp(i\omega t)$, we find from equations (5), (7) and (8)

$$\frac{\hat{\varrho}}{\varrho_0}=-\frac{1}{i\omega s}\left\{\hat{v}'+\left(\frac{\varrho_0'}{\varrho_0}-\frac{B_0'}{B_0}\right)\hat{v}-\frac{i\Omega}{i\Omega+\gamma}\frac{\gamma\beta}{2}\frac{N_0^2}{g}\hat{v}\right\}, \tag{10}$$

$$\frac{\hat{p}}{p_0}=-\frac{\gamma}{i\omega s}\frac{i\Omega+\chi_\varrho}{i\Omega+\gamma}\left\{\hat{v}'+\left(\frac{\varrho_0'}{\varrho_0}-\frac{B_0'}{B_0}\right)\hat{v}+\frac{i\Omega}{i\Omega+\chi_\varrho}\frac{N_0^2}{g}\hat{v}\right\}, \tag{11}$$

where $\Omega=\gamma\omega\tau_r$,

$$c_0^2=\frac{\gamma p_0}{\varrho_0}, \qquad N_0^2=-\frac{\varrho_0'}{\varrho_0}g-\frac{g^2}{c_0^2}$$

and

$$s=1+\frac{\gamma\beta}{2}\frac{i\Omega+\chi_\varrho}{i\Omega+\gamma}.$$

The caps denote ampitudes of the perturbations and the primes denote derivatives with respect to z. The quantities N_0 and c_0 refer to the Brunt – Väisälä frequency and sound speed in the unperturbed medium respectively.

Substituting equations (10) – (11) into equation (6), we obtain the following differential equation

$$Y'+\left(\frac{g}{c_0^2}\frac{i\Omega+\gamma}{i\Omega+\chi_\varrho}-\frac{Z'}{Z}\right)Y+\frac{\varrho_0}{i\omega}Z\left(\omega^2-\frac{i\Omega}{i\Omega+\chi_\varrho}N_0^2\right)\hat{v}=0, \tag{12}$$

where

$$Y=\frac{dv}{dz}+\left(\frac{\varrho_0'}{\varrho_0}-\frac{B_0'}{B_0}\right)\hat{v}+\frac{i\Omega}{i\Omega+\chi_\varrho}\frac{N_0^2}{g}\hat{v},$$

$$Z=\frac{i\omega}{\varrho_0 c_0^2}\left(\frac{\gamma}{2}\beta+\frac{i\Omega+\gamma}{i\Omega+\chi_\varrho}\right).$$

Further simplification of equation (12) yields

$$\left(\frac{\Lambda_0}{\Lambda_0'}\right)^2\hat{v}''+L\left(\frac{\Lambda_0}{\Lambda_0'}\right)\hat{v}'+\left(M\frac{\Lambda_0}{\Lambda_0'}+N\right)\hat{v}=0, \tag{13}$$

where

$$L=\frac{1}{\Lambda_0'}\left[-\frac{1}{2}+\frac{\gamma'}{\gamma}\Lambda_0 X-\frac{1}{i\Omega+\chi_\varrho}\{\Lambda_0'\chi_\varrho+(\chi_\varrho-1)\}\right],$$

$$M=\frac{1}{\Lambda_0'}\left[\frac{\gamma'}{\gamma}\left\{\frac{1}{\gamma}+X\left(\frac{1}{2}-\frac{1}{\gamma}\right)\right\}+\frac{\omega^2}{\gamma g}\left(1+\frac{\gamma\beta}{2}\right)+\frac{1}{i\Omega+\chi_\varrho}\right.$$
$$\left.\times\left\{-\Lambda_0''\chi_\varrho-\frac{\gamma'}{\gamma}\chi_\varrho\left(\frac{1}{\gamma}+n^2X\right)+\left(\frac{\gamma-\chi_\varrho}{\gamma}\right)\frac{\omega^2}{g}\right\}+\frac{n^2 i\Omega}{(i\Omega+\chi_\varrho)^2}\chi_\varrho\left(\frac{i\Omega'}{i\Omega}-\frac{\chi_\varrho'}{\chi_\varrho}\right)\right],$$

$$N=\frac{1}{\Lambda_0'^2}\left[-\frac{n^2}{2}(1+\beta)+\frac{1}{i\Omega+\chi_\varrho}\left\{\chi_\varrho\Lambda_0'\left(1+\frac{\beta}{2}\right)+\Lambda_0'^2\chi_\varrho+\left(\frac{\gamma-\chi_\varrho}{2\gamma}\right)\right.\right.$$
$$\left.\left.\times(1+\beta)+(\chi_\varrho-1)\left(1+\frac{\beta}{2}+\Lambda_0'\right)\right\}\right],$$

$$X=\frac{w-(\gamma/\gamma')w'}{w+\gamma\beta/2}$$

$\Lambda_0=p_0/\varrho_0 g$, $n^2=(\gamma-1)/\gamma+\Lambda_0'$ and $W=(i\Omega+\gamma)/(i\Omega+\chi_\varrho)$.

As it stands, equation (13) is best solved numerically. Before attempting this, however, it is instructive to simplify this equation so that an analytic solution is possible.

3 Polytropic atmosphere

Let us assume that the scale height in the equilibrium state varies linearly with height, so that

$$\Lambda_0(z)=\Lambda_0(0)+z\Lambda_0',$$

where Λ_0' is a constant. Such a state corresponds to a polytrope with index $1/(\Lambda_0'+1)$. We also assume that γ, μ and τ_r are constants. With these approximations the coefficients of $\hat{v}$ appearing in equation (13) become constants, given by

$$L=-\frac{1}{2\Lambda_0'}-\frac{1}{i\Omega+1},$$

$$M=\frac{\omega^2}{\gamma g\Lambda_0'}\left(1+\frac{\gamma\beta}{2}\right)+\left(\frac{\gamma-1}{i\Omega+1}\right)\frac{\omega^2}{\gamma g\Lambda_0'},$$

$$N=-\frac{n^2}{2\Lambda_0'^2}(1+\beta)+\frac{1}{(i\Omega+1)}\frac{1}{\Lambda_0'^2}\left\{\left(1+\frac{\beta}{2}\right)+\Lambda_0'^2+\left(\frac{\gamma-1}{2\gamma}\right)(1+\beta)\right\}.$$

Equation (13) is now identical to equation (10) of Webb & Roberts (1980) and admits the formal solution

$$\hat{v}=p^{1-L}\{AJ_s(p)+BY_s(p)\} \tag{14}$$

where $p^2=4M\Lambda_0/\Lambda_0'$ and $s^2=(1-L)^2-4N$.

The quantities A and B are constants to be determined by the boundary conditions. We assume a no-flow boundary condition, so that $\hat{v}$ is zero at $z=0$ and $z=z_1$. Substituting these conditions

in equation (14), the condition for the existence of a non-trivial solution yields

$$J_s\{p_0(0)\}\, Y_s\{p(z_1)\} - J_s\{p(z_1)\}\, Y_s\{p(0)\} = 0. \tag{15}$$

Equation(15) can now be used to determine the eigenfrequencies ω (in general complex). We consider first the adiabatic limit.

3.1 ADIABATIC CASE

Defining $q = 1/\tau_r$, the adiabatic limit corresponds to $q = 0$. This limit has been examined by Webb & Roberts (1978) and the interested reader can refer to this paper for more details. We assume that s is real and for convenience consider only integral values n (this can be arranged by choosing a suitable combination of Λ_0' and γ). Thus, a determination of ω reduces to determining the zeros of the function F_n, given by

$$F_n = J_n\{p(0)\}\, Y_n\{\lambda p(0)\} - J_n\{\lambda p(0)\}\, Y_n\{p(0)\},$$

where $\lambda = p(z_1)/p(0) = 1 + z_1\Lambda_0'/\Lambda_0$.

It is well known that F_n has an infinity of zeros, all of which are positive and real (e.g. Abramowitz & Stegun 1965). The eigenfrequencies $\pm\omega_n$ are therefore real and ordered as follows

$$|\omega_1| < |\omega_2| < \ldots < |\omega_n| < \ldots$$

3.2 RADIATIVE EXCHANGE INCLUDED

We assume that τ_r is large enough so that q can be treated as a first order quantity. Defining $\omega = \omega_a + i\chi$, where a denotes the adiabatic limit, χ is in general at least of order q. Let us expand all quantities about the adiabatic state ($q = 0$) and retain only terms to first order in q and χ. Thus, for example

$$J_s(p) \approx J_n(p_a) + \frac{i}{\omega_a}\left\{(\chi - q)\frac{\gamma-1}{2}\frac{1}{(\gamma\beta/2+1)}\frac{\partial J_n}{\partial n} - \frac{q}{\gamma}\frac{s_1^2}{n}\frac{\partial J_n}{\partial p_a}\right\}, \tag{16}$$

where

$$s = \sqrt{s_a^2 + s_1^2} \approx n + \frac{q}{i\gamma\omega_a}\frac{s_1^2}{n},$$

and

$$s_1^2 = 1 + \frac{1}{2\Lambda_0'} - \frac{2}{\Lambda_0'^2}\left\{\frac{\gamma-1}{2\gamma}(1+\beta) + \Lambda_0'\left(1+\frac{\beta}{2}\right) + \Lambda_0'^2\right\}.$$

Substituting equation (16) (and a similar one for Y_s) into equation (15), we can determine χ, which is given by

$$\chi_n = \frac{q}{\gamma}\left\{\frac{\gamma-1}{2}\frac{1}{(\gamma\beta/2+1)} + \frac{s_1^2}{n}\frac{a}{b}\right\}, \tag{17}$$

where

$$a=\frac{\partial J_n(p_0)}{\partial n}Y_n(p_1)+\frac{\partial Y_n(p_1)}{\partial n}J_n(p_0)-\frac{\partial Y_n(p_0)}{\partial n}J_n(p_1)-\frac{\partial J_n(p_1)}{\partial n}Y_n(p_0),$$

$$b=p_0\{J_n'(p_0)\,Y_n(p_1)-Y_n'(p_0)J_n(p_1)\}+p_1\{Y_n'(p_1)J_n(p_0)-J_n'(p_1)\,Y_n(p_0)\}$$

$p_0\equiv p_a(0)$

and

$p_1=p_a(z_1)$.

4 Real atmosphere

We consider first an equilibrium atmosphere based on the VAL/SP model (taken from Spruit 1977) for the temperature. Equations (1)–(3) (along with Saha's equation to determine μ) were then used to determine the equilibrium quantities. The thermodynamic quantities like C_v were determined following Mihalas (1967) and the opacities were calculated by interpolating from a table by Kurucz (1979). In Table 1 the z variation of some of the equilibrium quantities is presented. It may be noted that τ_r is depth dependent and that radiative exchange is most efficient for $z\lesssim -100$ km.

Equation (13) was solved numerically by approximating the derivatives by finite differences. A closed boundary condition ($\hat{v}=0$) was applied at the lower boundary. However, for the upper boundary both closed as well as open boundary conditions corresponding to $\hat{v}=0$ and $\hat{v}'=0$ were adopted. Inserting the boundary conditions in the difference equations led to a homogeneous tridiagonal system of equations which constituted a generalized eigenvalue problem. The eigenvalues were determined by finding the roots of a determinantal equation. Since we anticipated complex roots, numerical algorithms for locating complex roots, for efficiently evaluating determinants and finally for calculating eigenvectors were required. The choices of an interval-bisection algorithm for real roots and Müller's method for complex roots proved extremely satisfactory. Determinants were evaluated using Gaussian elimination with partial pivoting and the eigenvectors were calculated using inverse iteration (Wilkinson & Reinsch 1971). Once $\hat{v}$ was determined, $\hat{\varrho}$ and $\hat{p}$ were calculated using equations (10)–(11) and $\hat{T}$ was then determined from the relation

$$\frac{\hat{T}}{T_0}=\frac{1}{\chi_T}\left(\frac{\hat{p}}{p_0}-\chi_\varrho\frac{\hat{\varrho}}{\varrho_0}\right). \tag{17}$$

A uniform grid with a spacing of 10 km was used in all computations. This was sufficiently fine to resolve the steepest of gradients. In the majority of cases, the upper and lower boundaries were placed at 500 and -2000 km, respectively, where the $z=0$ level was chosen to coincide with $\tau_{5000}=1$ in the external medium.

5 Results

5.1 POLYTROPIC ATMOSPHERE

In Table 2 the real and imaginary parts of the eigenfrequencies $\omega_{n,m}$ and $\chi_{n,m}$, where m denotes the order of the zero of F_n ($m=1$ corresponds to the fundamental mode) are presented for different n assuming $\gamma=1.2$, $\beta=1/\gamma$, $q=10^{-3}\,s^{-1}$ and $z_1=-2000$ km. The quantity $p_{n,m}$ in the table satisfies $F_n(p_{n,m})=0$. For purposes of comparison, we also present the eigenfrequencies

Table 1. Equilibrium quantities at different heights in a solar flux tube for $\beta=3$, and $a_{00}=100$ km.

z(km)	T_0(K)	ρ_0(gm cm^{-3})	B_0(G)	a_0(km)	κ(gm cm^{-2})	τ_r(s)
500	$4.15.10^3$	$4.23.10^{-9}$	97	309	$4.46.10^{-3}$	332
300	$4.52.10^3$	$2.57.10^{-8}$	250	192	$2.42.10^{-2}$	47
100	$5.29.10^3$	$1.28.10^{-7}$	603	122	$1.26.10^{-1}$	8
0	$6.27.10^3$	$2.28.10^{-7}$	876	100	18	6
-100	$8.69.10^3$	$2.89.10^{-7}$	$1.17.10^3$	89	88	149
-300	$1.11.10^4$	$4.75.10^{-7}$	$1.75.10^3$	72	200	$4.3.10^3$
-500	$1.25.10^4$	$7.63.10^{-7}$	$2.42.10^3$	61	515	$1.9.10^4$
-1000	$1.50.10^4$	$2.08.10^{-6}$	$4.61.10^3$	44	$1.85.10^3$	$1.9.10^5$

(denoted by bars), obtained using the boundary condition $\hat{v}'=0$ at the upper boundary. The critical value of Λ_0' for the onset of instability based on Schwarzschild's criterion is $\Lambda_{0,\,\mathrm{crit}}'=-(\gamma-1)/\gamma=-0.1667$ for $\gamma=1.2$. Thus, for $n=1$ the equilibrium would be unstable in the absence of a magnetic field, whereas states with higher n would be stable. The fact that the equilibrium for $n=1$ is stable (in the absence of heat exchange) is possible owing to the presence of a sufficiently strong magnetic field. Radiative heat exchange, however, can destabilize the equilibrium and lead to overstable behaviour. This, indeed, is the case for $n=1$ and 2 (for the fundamental mode), since χ is negative. For higher n, however, heat exchange leads to damped oscillations. For small values of n (i.e. large Λ_0'), the growth rate χ is higher owing to a steeper

Table 2. Real and complex frequencies $\omega_{n,m}$ and $\chi_{n,m}$ respectively for various n and m, where m denotes the order of the harmonic for fixed n, assuming $\gamma=1.2, \beta=1/\gamma$ and $q=10^{-3}$(s^{-1}). The prime quantities correspond to the boundary condition $\hat{v}'_{\mathrm{top}}=0$.

n	Λ_0'	m	$p_{n,m}$	$\omega_{n,m}$ (s^{-1})	$\chi_{n,m}$ (s^{-1})	$\bar{\omega}_{n,m}$ (s^{-1})	$\bar{\chi}_{n,m}$ (s^{-1})
		1	3.81	$1.13.10^{-2}$	$-4.29.10^{-5}$	$8.31.10^{-3}$	$-1.44.10^{-4}$
1	-0.1798	2	7.55	$2.23.10^{-2}$	$1.92.10^{-5}$	$1.81.10^{-2}$	$-4.35.10^{-6}$
		1	4.23	$1.16.10^{-2}$	$-7.59.10^{-6}$	$9.20.10^{-3}$	$-5.51.10^{-5}$
2	-0.1667	2	8.11	$2.22.10^{-2}$	$2.77.10^{-5}$	$2.85.10^{-2}$	$3.27.10^{-5}$
		1	4.84	$1.20.10^{-2}$	$3.23.10^{-5}$	$9.80.10^{-3}$	$2.46.10^{-5}$
3	-0.1510	2	8.91	$2.21.10^{-2}$	$3.88.10^{-5}$	$2.82.10^{-2}$	$3.97.10^{-5}$
		1	5.57	$1.24.10^{-2}$	$6.84.10^{-5}$	$1.06.10^{-2}$	$8.33.10^{-5}$
4	-0.1360	2	9.86	$2.20.10^{-2}$	$5.05.10^{-5}$	$2.80.10^{-2}$	$4.73.10^{-5}$
		1	6.37	$1.29.10^{-2}$	$9.86.10^{-5}$	$1.12.10^{-2}$	$1.25.10^{-4}$
5	-0.1227	2	10.90	$2.20.10^{-2}$	$6.19.10^{-5}$	$2.78.10^{-2}$	$5.47.10^{-5}$

temperature gradient, or a greater degree of superadiabaticity, which, of course, drives the instability.

A comparison between the instability growth rates for the boundary conditions $\hat{v}=0$ and $\hat{v}'=0$ at $z=0$ shows that the growth rate is faster in the latter case. An interesting feature to note is that for $n=1$, both the fundamental and first harmonic turn out to be unstable.

5.2 REAL ATMOSPHERE

We now describe the results for the case of the solar stratification using a realistic heat exchange time constant τ_r. For reasons of computational economy, only eigenvalues and eigenvectors corresponding to the fundamental mode were calculated. In order to check the numerical procedure and also to find a satisfactory location for the lower boundary, the adiabatic case was also treated. A comparison with the results of Spruit & Zweibel (1979), who treated this case using the full depth of the convection zone and an upper boundary at $z=500$ km, showed a remarkable agreement (to within 10 per cent). However, we used a lower boundary at $z=-2000$ km which *a posteriori* justified this choice. Fig. 1 depicts the variation of $\eta=i\omega$ with β, for the adiabatic case and also for different values of a_{00}, where a_{00} denotes the radius of the tube

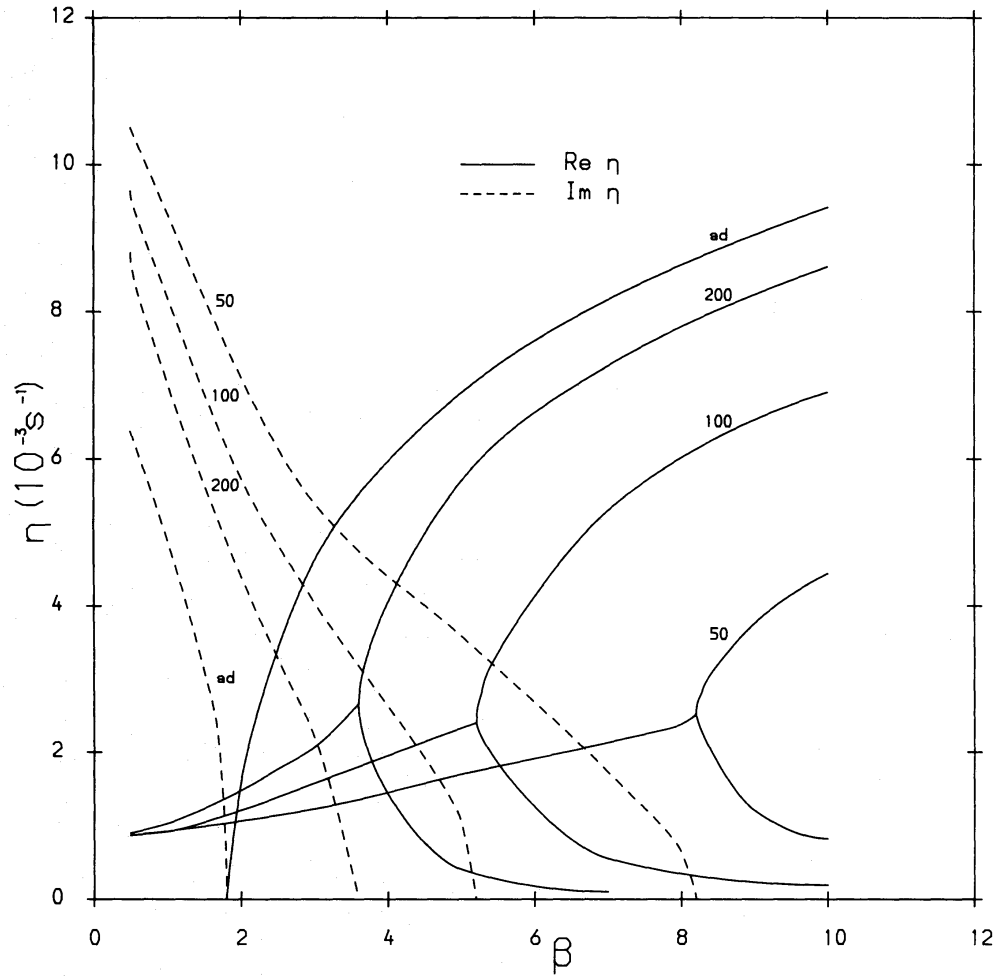

Figure 1. The variation of the complex growth rate η as a function of β. The symbol ad refers to the adiabatic case and the numbers denote the value of a_{00} used when radiative exchange is included. Full and dashed lines correspond to real and imaginary values respectively of η.

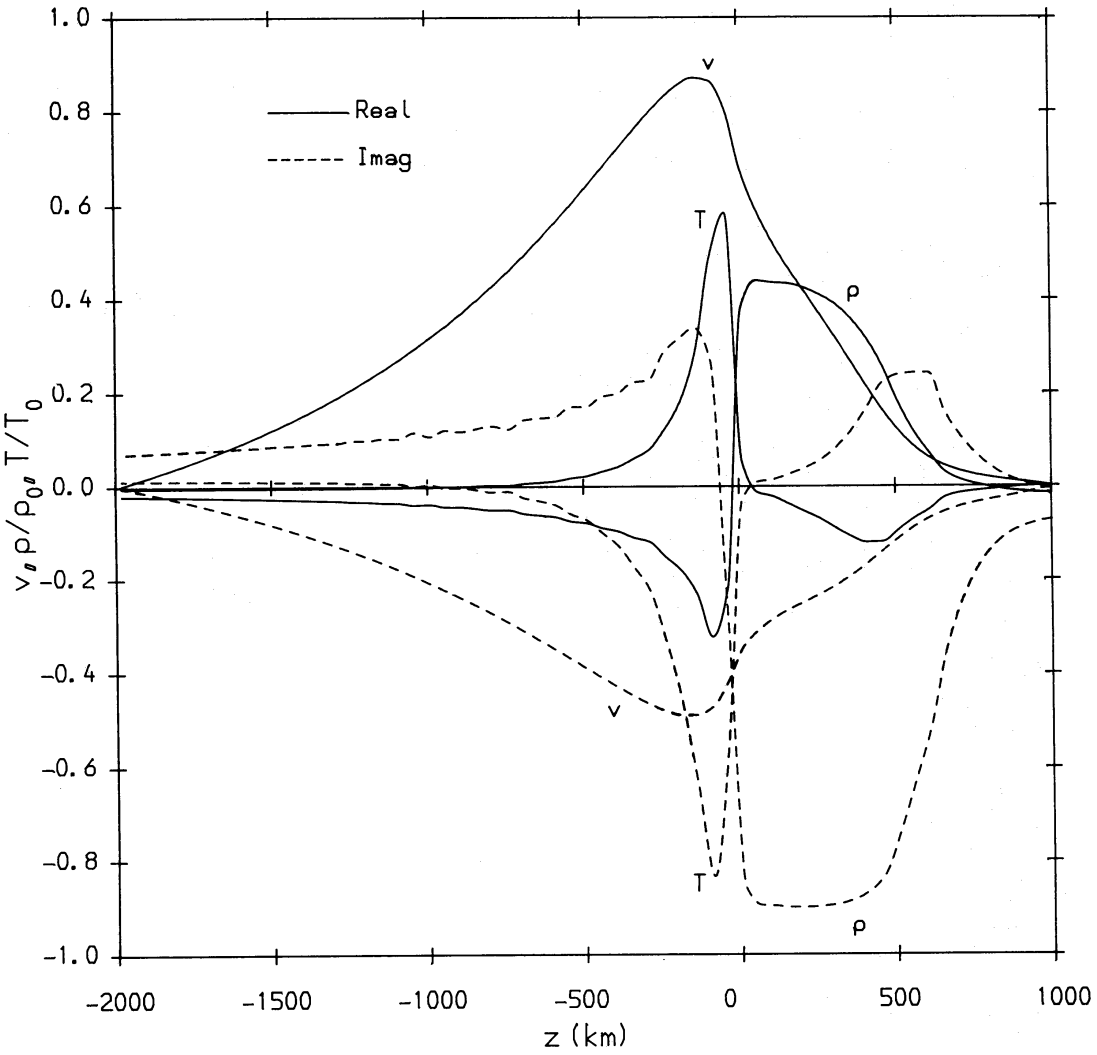

Figure 2. The variation of $\hat{v}$, $\hat{\varrho}/\varrho_0$ and $\hat{T}/T_0$ with z for $a_{00}=200$ km and $\beta=3$. Each value has been normalized with respect to the maximum value in the interval. Full and dashed lines are used for real and imaginary parts respectively of the eigenvectors.

at $z=0$ in the equilibrium state. Let us first examine the adiabatic case, where the frequency only appears as ω^2 (thus ω and $-\omega$ are both eigenvalues). For $\beta>\beta_c$, where β_c denotes some critical value, $\eta^2>0$ and the system is unstable with a growth rate that increases with β. For $\beta<\beta_c$, where $\beta_c\simeq1.8$, the equilibrium is stable with an oscillation frequency that increases with decreasing β.

In the general case, η is complex with roots occurring in complex conjugate pairs. From Fig. 1 we note that for each value of a_{00}, it is possible to distinguish between modes which are purely growing (i.e. for which Im $\eta=0$) and those which are overstable. When $\beta<\beta_c$, where β_c depends upon a_{00}, the system is overstable with a growth rate and oscillation frequency which increase and decrease respectively with β. At $\beta=\beta_c$, a bifurcation into two purely unstable modes occurs. The growth rate of the upper branch (the fast mode) increases with β whereas the growth rate of the lower branch (the slow mode) decreases with increasing β. Similar behaviour was also noted by Spruit (1979b, unpublished). We also explored the possibility that for low β there may exist a second critical value below which the system is stable. Such an attempt proved futile; no matter how small the value of β, overstability was invariably present.

Fig. 2 shows the variation with z of $\hat{v}$, $\hat{\varrho}/\varrho_0$ and $\hat{T}/T_0$ (all quantities normalized with respect to the absolute maximum value in the flux tube) for $a_{00}-200$ km and $\beta=3$. An upper boundary at

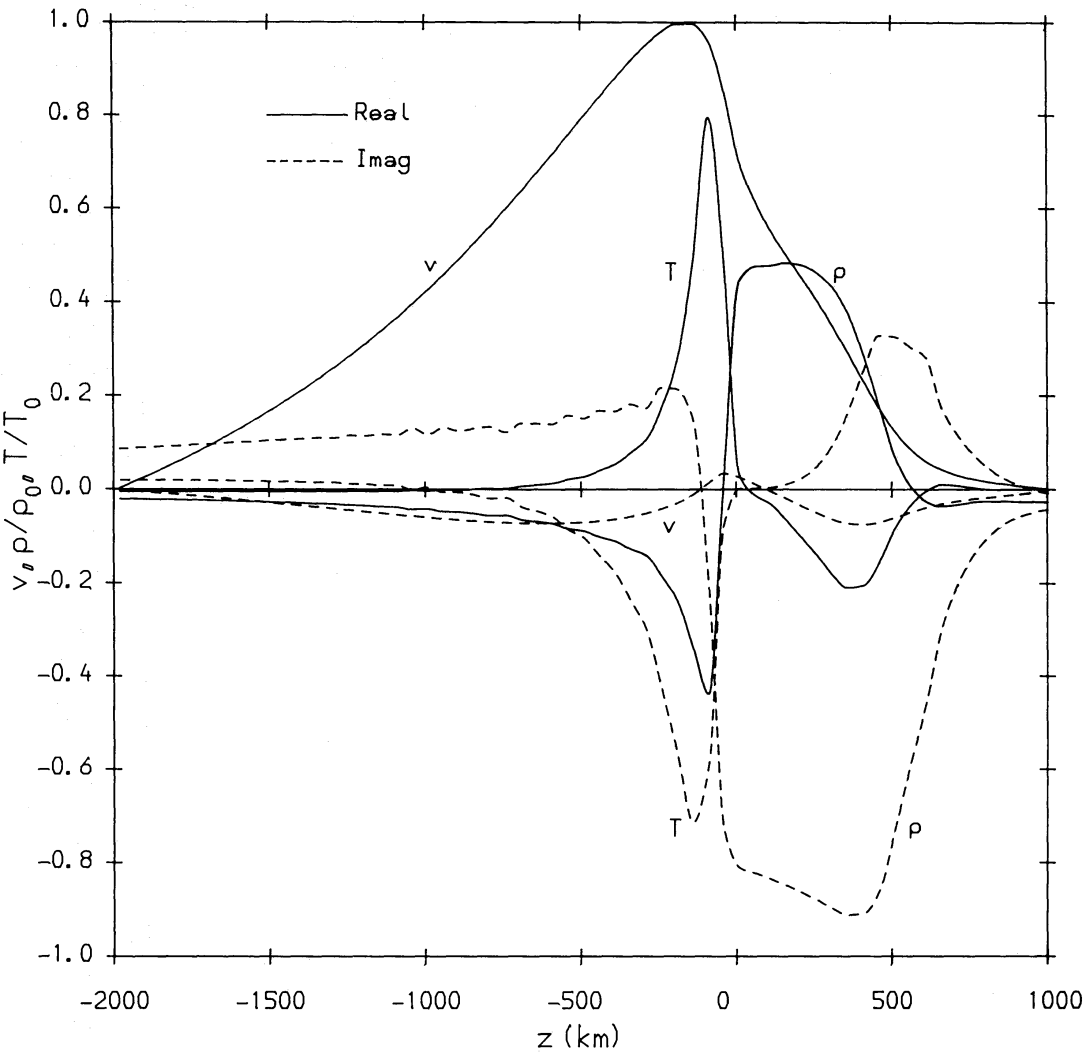

Figure 3. The variation of $\hat{v}$, $\hat{\varrho}/\varrho_0$ and $\hat{T}/T_0$ with z for $a_{00}=100$ km and $\beta=3$. Each value has been normalized with respect to the maximum value in the interval. Full and dashed lines are used for real and imaginary parts respectively of the eigenvectors.

$z=1000$ km was used. The absence of any nodes in the curve for $\hat{v}$ may be noted. Furthermore, we see that the largest contribution to $\hat{v}$ occurs in some 1000 km below $z=0$, the region of largest superadiabaticity. Deeper down in the flux tube, $\hat{v}$ becomes extremely small due to the temperature gradient tending to the adiabatic value, thus reducing the force driving the instability. The density and temperature perturbations $\hat{\varrho}/\varrho_0$ and $\hat{T}/T_0$, in contrast to $\hat{v}$, reverse signs around $z\simeq 0$. At $z\simeq 0$, the stratification changes from subadiabatic to superadiabatic. It is also worthwhile to note that both Re $\hat{\varrho}/\varrho_0$ and Re $\hat{T}/T_0$ become negligibly small close to the boundaries.

Fig. 3 again shows the z variation of the eigenvectors, but this time for $a_{00}=100$ km, i.e. for a thinner flux tube. The qualitative behaviour is the same as in Fig. 2, except that since the growth rates are different in the two cases, the ampitudes and phases of the perturbations are different.

Figs 4 and 5 show the z dependence of Φ_T, Φ_v, $\Phi_T-\Phi_v$ where Φ_T and Φ_v denote the phases of the temperature and velocity oscillations respectively, for $a_{00}=200$ km and $a_{00}=100$ km respectively. In both cases, the phase difference between T and v depicts a sharp-change at $z\simeq 0$, but for $z\gtrless 0$ the variation is fairly gradual. The sharp behaviour of $\Phi_T-\Phi_v$ at $z\simeq 0$ is due to Φ_T since Φ_v varies rather smoothly over the entire z interval.

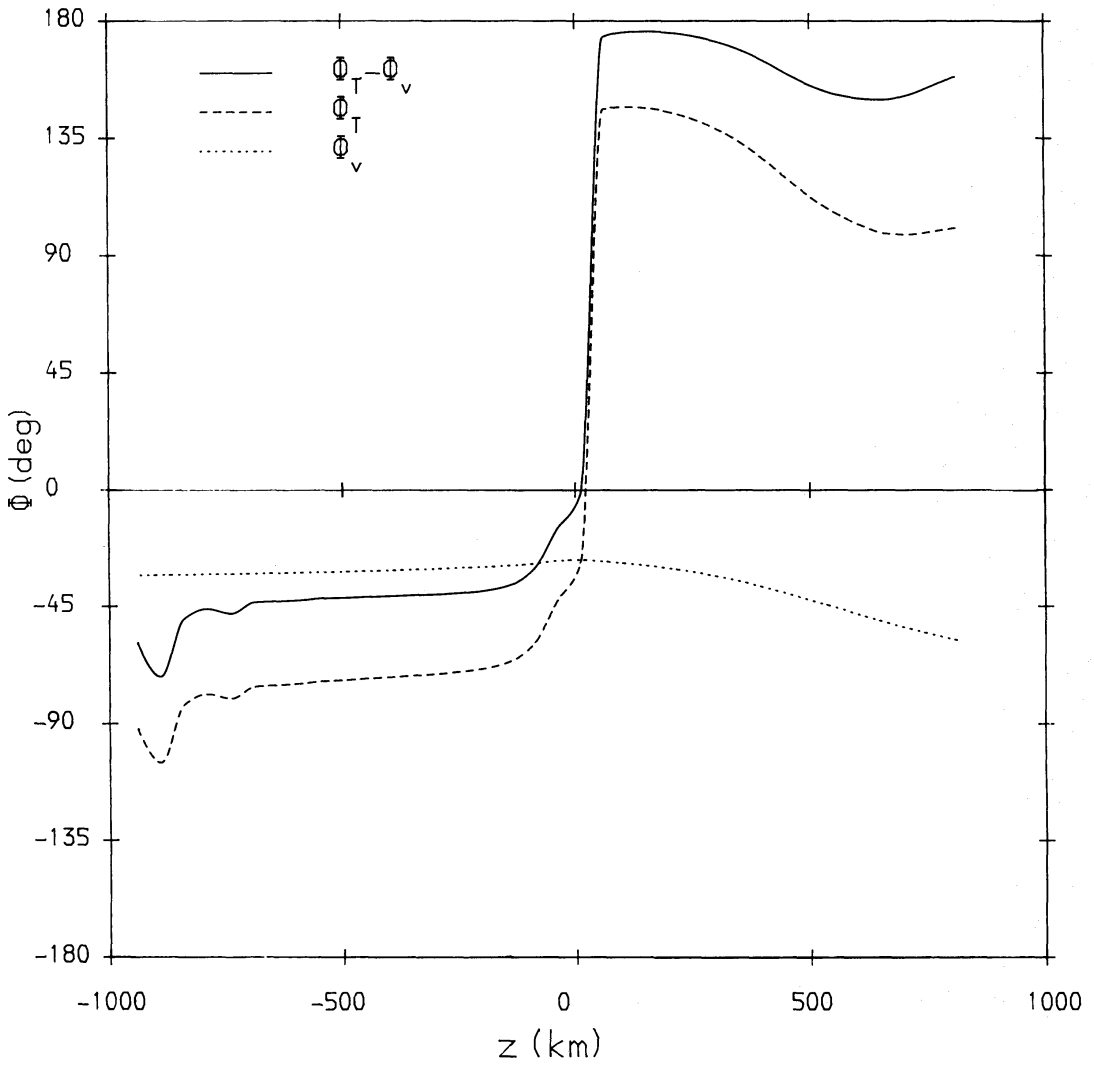

Figure 4. The z dependence of the phases Φ_T (dashed line), Φ_v (dotted line) and $\Phi_T-\Phi_v$ (full line) for $a_{00}=200$ km and $\beta=3$.

We now turn to the sensitivity of the results on the boundary conditions as well as on the location of the boundaries. It was found that moving the lower boundary from $z=-2000$ km to $z=-5000$ km had a negligible influence on the eigenvalues. We, thus, chose only to consider the effect of varying the upper boundary condition. In Tables 3 and 4, the complex growth rates (η_r, η_i) are shown for various locations of the top boundary for two values of β. The difference between the two tables is that they correspond to the boundary conditions $\hat{v}_{top}=0$ and $\hat{v}'_{top}=0$. We observe that the difference between the eigenvalues for $z_{top}=1000$ km and $z_{top}=500$ km is, for all practical purposes, rather marginal, for both types of boundary conditions. However, moving the

Table 3. The complex growth rates (s^{-1}) for different β and various locations of z_{top}, assuming $\hat{v}_{top}=0$ and $a_{00}=100$ km.

β	z_{top}=1000km	z_{top}=500km	z_{top}=0
10	$(7.10,0).10^{-3}$	$(6.90,0).10^{-3}$	$(0.74,3.03).10^{-3}$
	$(1.51,0).10^{-4}$	$(1.86,0).10^{-4}$	
3	$(1.58,3.78).10^{-3}$	$(1.58,4.04).10^{-3}$	$(0.03,9.25).10^{-3}$

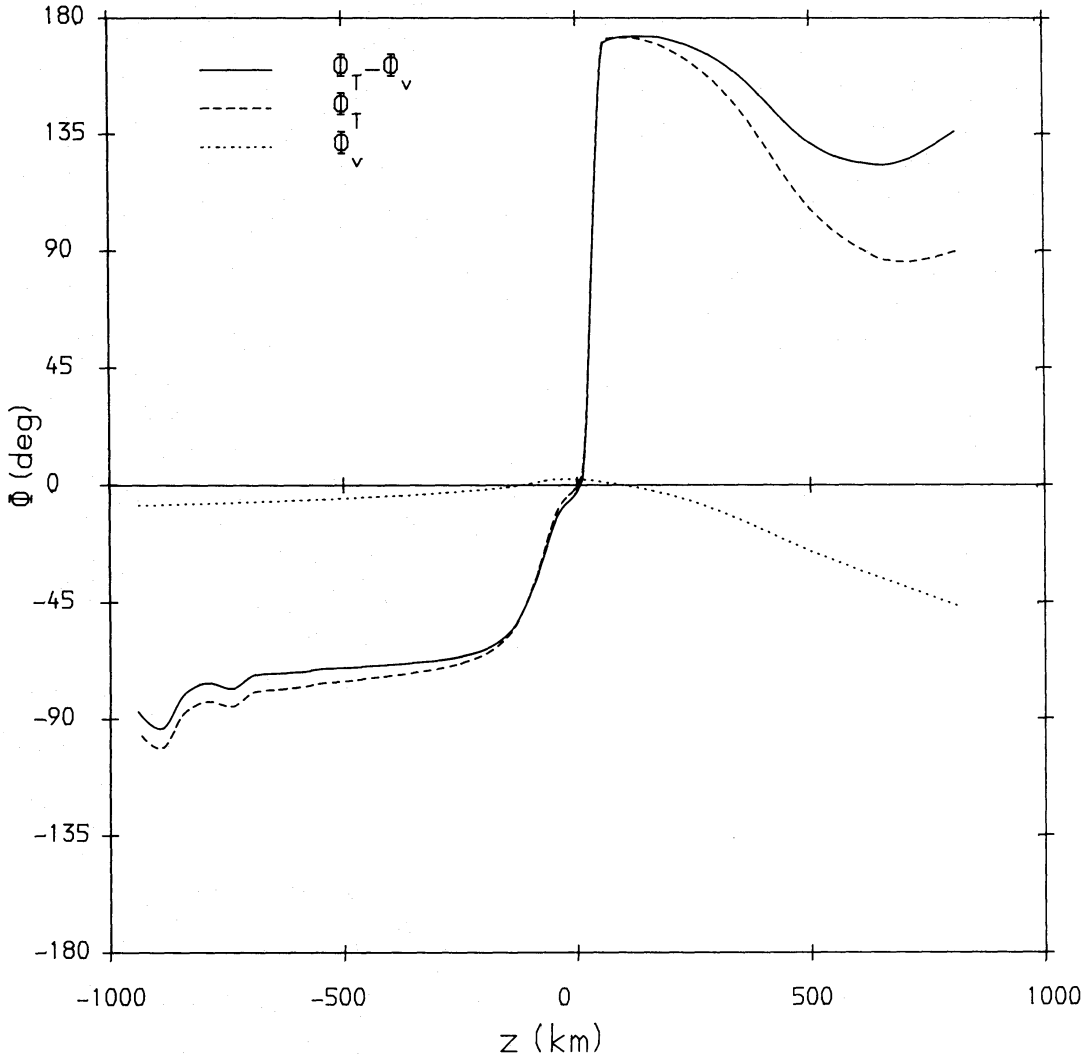

Figure 5. The z dependence of the phases Φ_T (dashed line), Φ_v (dotted line) and $\Phi_T-\Phi_v$ (full line) for $a_{00}=100$ km and $\beta=3$.

upper boundary to $z=0$, leads to an appreciable change in η for $\hat{v}_{top}=0$. In fact, in the latter case, the purely growing modes, found earlier for $\beta=10$, are now unstable! On the other hand, the open boundary condition turns out to be not so bad, giving eigenvalues which agree roughly with the previous cases.

6 Discussion

The results presented in the previous sections exhibit several interesting features. We have found that an equilibrium which in the absence of heat exchange is stable (against the convective

Table 4. The complex growth rates (s^{-1}) for different β and various locations of z_{top}, assuming $\hat{v}'_{top}=0$ and $a_{00}=100$ km.

β	z_{top}=1000km	z_{top}=500km	z_{top}=0
10	(7.10,0).10^{-3}	(6.90,0).10^{-3}	(8.33,0).10^{-3}
	(1.51,0).10^{-4}	(1.65,0).10^{-4}	(1.64,0).10^{-4}
3	(1.58,3.78).10^{-3}	(1.49,3.85).10^{-3}	(2.03,3.72).10^{-3}

instability) can become overstable in its presence. This behaviour can be discerned both for polytropic as well as for real atmospheres. Similar behaviour was also noted by Syrovatskii & Zhughzda (1968) for an associated problem. They also found that for certain values of the polytropic index, the criterion for overstability is less stringent than the Schwarzschild one. In the case of the solar stratification, a flux tube, which is thermally insulated, can be stable even though the temperature gradient inside it is superadiabatic (Spruit & Zweibel 1979, see also Webb & Roberts 1978). Thus, if adiabatic conditions were to prevail, one would expect vertical undamped oscillations (in time) in intense flux tubes. In the presence of radiative exchange, however, oscillations, whose amplitudes grow in time, are now possible.

Let us now consider the variation of η with β for different values of a_{00} (i.e. the variation of the eigenfrequencies with the strength of the magnetic field for tubes with different radii). Since the heat exchange time τ_r depends upon the tube radius, decreasing a_{00} leads to a decrease in τ_r in the optically thick layers ($\varkappa\rho_0 a_0 \geqslant 1$), which also correspond to the superadiabatic region. Thus, we expect the destabilizing effect to be greatest for tubes with smaller radii and consequently the growth rate to decrease with a_{00}. It may be worthwhile to mention here that in the subadiabatic layers ($z>0$), the flux tube is optically thin and τ_r becomes independent of a_{00}. The frequency $\omega = i\eta_r$ of the oscillations, on the other hand, increases with β. This can be understood by noting that the oscillation period ($\sim 1/\omega$) is inversely proportional to the tube speed c_t, the typical speed at which disturbances propagate in the medium. Using the relationship

$$c_t = \frac{c_s}{\sqrt{(\gamma\beta/2+1)}}$$

we find that a decrease in β leads to an increase in c_t and consequently to an increase in ω.

An interesting feature of the solutions is the existence of a critical value of β at which a bifurcation occurs from overstability to two purely growing modes. It may be mentioned that the latter do not represent different harmonics of the same mode, but in fact correspond to two different types of modes. This can also be discerned by checking the velocity eigenvectors for the absence of nodes. By comparing with the adiabatic case, we identify the fast mode as a convective mode, modified by heat exchange. The slow mode seems to be a new mode which is introduced by the inclusion of radiative effects. When $\beta > \beta_c$, the system is monotonically unstable. Physically, we can understand this by noting that the occurrence of overstability is related to the fact that the tube can exchange heat with the ambient medium. Now, the time scale for convective instability τ_{conv} decreases with increasing β, whereas τ_r increases with β (since $\tau_r \sim B^{-1}$ for $z>0$). Thus, when the magnetic field is weak or β is large, radiative exchange plays an insignificant role and one expects instability, similar to the adiabatic case. The critical value β_c corresponds to the situation $\tau_{conv} \approx \tau_r$. We also found that for β very small ($\beta \ll \beta_c$), there does not appear to exist a second critical value of β below which stability occurs. This is possibly related to the fact that a decrease of β leads to an even stronger influence of heat exchange on the vertical motions in the flux tube.

Turning our attention to the eigenvectors, we find that the density and temperature perturbations undergo a reversal of sign at $z \simeq 0$. Writing $\hat{f} = |\hat{f}| \exp(i\Phi)$, where f denotes a perturbed quantity, the sign of $\hat{f}$ depends upon the sign of $\cos\Phi$. In the superadiabatic region ($z \lesssim 0$) $\hat{T}$ and $\hat{\varrho}$ are positive and negative respectively, whereas in the subadiabatic region ($z \gtrsim 0$), $\hat{T}$ and $\hat{\varrho}$ have opposite signs. In order to see why this happens, let us consider a velocity perturbation which produces a unidirectional flow in the flux tube. Let us assume that we have a downflow ($v<0$), which in superadiabatic layers brings hotter material downwards. If there is approximate horizontal pressure balance, this material will be denser than its surroundings. For the subadiabatic layers the opposite situation occurs.

The phases of the perturbations also provide interesting information. In the adiabatic case, $\hat{v}$ is always real and hence its phase $\Phi_v=0$, which means that in the stable case, only vertical motions corresponding to standing oscillations can occur. For the general case, $\Phi_v\neq 0$. Since Φ_v varies (albeit not strongly) with z, we have propagating oscillations. Furthermore, these oscillations can transport energy. To second order, the only contribution to the time-averaged energy flux at some height comes from the enthalpy flux $\sim\langle vp\rangle$ (there is no first order contribution as $\langle v\rangle=0$). For the overstable case $\langle vp\rangle=|\hat{v}||\hat{p}|\cos(\Phi_v-\Phi_p)\neq 0$ and hence the energy flux is finite. In the stable adiabatic case, $\Phi_v-\Phi_p=0$ and, therefore, there is no energy transport.

We consider next the effect of boundary conditions on the results. We found that for an upper boundary condition at $z=0$, closed and open boundary conditions gave completely different results. The reason is not hard to see. Since $z=0$ is located at a height where the temperature gradient becomes superadiabatic, the velocity amplitude tends to be large there. Using a closed boundary condition effectively decreases the length of the superadiabatic region, thus reducing the growth rate. On the other hand, the boundary condition $\hat{v}'_{top}=0$ provides a less retrictive limitation on $\hat{v}$ and in fact yields a fairly reasonable condition. The differences in the eigenvalues for $z_{top}=1000$ km and $z_{top}=500$ km are rather marginal as these levels are situated sufficiently far from the region driving the instability. This is also borne out by Figs 2 and 3, which show that $\hat{v}$ drops off fairly rapidly with height, becoming negligibly small for $z\gtrsim 500$ km.

Finally, let us compare the results for the polytropic case with those for the realistic case, bearing in mind that the solar stratification cannot be accurately described by the polytropic approximation over the entire height range as well as the fact that τ_r is far from constant. Nevertheless, a comparison between the fundamental in Table 2 for $\Delta'_0=-0.18$ (for $\hat{v}'_{top}=0$) and the corresponding case for $\beta=0.8$ in Fig. 1 gives a reasonable agreement for the period. Agreement between the growth rates can be adjusted by choosing an appropriate value of q (see equation 17). Strictly, speaking this is not consistent when the growth rate becomes comparable to the period.

An assumption that we have tacitly employed is the absence of flows in the initial equilibrium and the equality of temperatures between the flux tube and the external medium. Observationally, there is reason to believe that there are no systematic downflows in intense flux tubes (Stenflo & Harvey 1984), although the cause of asymmetries in their V profiles is not known. Equality of temperatures is not such a bad assumption in the surface layers, where the heat exchange time is rather small. In the very deep layers, this may not be valid. However, the amplitude of the perturbation is extremely small in these layers, and consequently the final results are unlikely to be greatly different.

7 Observational implications

We now discuss some of the observational implications arising out of our study for the Sun. It is useful to distinguish between the purely unstable case ($\beta\geq\beta_c$) and the overstable case ($\beta<\beta_c$). In the adiabatic case $\beta_c\cong 1.8$, which corresponds to a critical surface field ≈ 1100 G at $z=0$ for $p_e=1.3\times 10^5$ dyn cm^{-2}. However, in the more realistic case, when lateral heat exchange is allowed, β_c varies from about 3.6 for $a_{00}=200$ km to 8.2 for $a_{00}=50$ km, yielding critical fields of about 850 G and 600 G respectively. Thus, flux tubes with $\beta>\beta_c$ are unstable and will undergo convective collapse (Hasan 1984a, b). In this paper we are primarily interested in the overstable case. The periods and growth times of the oscillations lie typically in the range 650–1500 and 1150–625 s respectively for β in the range 0.5–3.0 assuming $a_{00}=100$ km. Unfortunately, no observations of oscillations in intense flux tubes to date have been reported, possibly owing to the difficulties associated with spatially resolving fine scale elements on the Sun. Thus, a comparison must await a future date, perhaps when space observations become available. What could be

verified from ground-based observations, however, are phase relationships between velocity–velocity (at two heights) and temperature–velocity fluctuations. The phase difference in velocities at $z=500$ km and $z=0$ varies from about 15° for $a_{00}=200$ km to 25° for $a_{00}=100$ km. On the other hand, the phase differences between temperature and velocity are about 155° and 130° respectively at $z=500$ km and approximately 180° close to $z=0$. For $z<0$, $\Phi_T-\Phi_v$ undergoes a reversal of sign, for reasons already pointed out, and after some 100 km levels to an almost constant value down to a depth of about 900 km.

8 Concluding remarks

The purpose of the present investigation was to examine the detailed nature of oscillatory behaviour that can occur in intense flux tubes. In order to keep the analysis sufficiently general we treated first a polytropic atmosphere under certain approximations for which an analytic solution was possible. We then solved the problem for a realistic stratification using model opacities so as to obtain results applicable to the Sun. Our results clearly indicate that states, which in the adiabatic limit are stable, can be driven overstable when heat exchange is included in the analysis. An interesting property of the solutions, which appears to be fairly general, is the existence of a bifurcation at $\beta=\beta_c$ from overstability into two purely growing modes. The fast mode resembles an ordinary convective mode, whereas the slow mode owes its existence to radiative effects. We also found it worthwhile to calculate eigenvectors from which phase relationships could be determined. It is hoped that these can be verified observationally in the not too distant future. Finally, we demonstrated that by a judicious choice of boundary locations, the results become insensitive to boundary conditions so that the analysis has rather general validity.

Acknowledgments

I am thankful to Dr H. Spruit for helpful discussions and for making available unpublished results. Financial assistance was provided by the Science and Engineering Research Council, UK.

References

Abramowitz, M. & Stegun, I. A., 1965. In: *Handbook of Mathematical Functions*, p. 358, Dover, New York.
Hasan, S. S., 1984a. *Astrophys. J.*, **285,** 851.
Hasan, S. S., 1984b. *Astr. Astrophys.*, **143,** 39.
Kurucz, R. L., 1979. *Astrophys. J. Suppl.*, **40,** 1.
Mihalas, D., 1967. In: *Methods in Comp. Phys.*, Vol. 7, eds Adler, B., Fernbach, S. & Rotenburg, M., Academic Press, New York.
Nordlund, Å., 1983. In: *Solar and Stellar Magnetic Fields, IAU Symp. No. 102*, ed. Stenflo, J. O., Reidel, Dordrecht, Holland.
Parker, E. N., 1978. *Astrophys. J.*, **211,** 368.
Roberts, B., 1976. *Astrophys. J.*, **204,** 268.
Roberts, B. & Webb, A. R., 1978. *Solar Phys.*, **56,** 5.
Spiegel, E. A., 1957. *Astrophys. J.*, **126,** 202.
Spruit, H., 1977. *PhD thesis*, University of Utrecht.
Spruit, H. & Zweibel, E., 1979. *Solar Phys.*, **62,** 15.
Spruit, H., 1979a. *Solar Phys.*, **61,** 363.
Spruit, H., 1982. *Solar Phys.*, **75,** 3.
Stenflo, J. O. & Harvey, J., 1984. *Solar Phys.*, **95,** 99.
Syrovatskii, S. I. & Zhugzhda, Y. D., 1968. *Soviet Astr. A.J.*, **11,** 945.
Webb, A. R. & Roberts, B., 1978. *Solar Phys.*, **59,** 249.
Webb, A. R. & Roberts, B., 1980. *Solar Phys.*, **68,** 87.
Wilkinson, J. H. & Reinsch, C., 1971. In: *Handbook for Automatic Computation*, Vol. 2, Springer-Verlag, Berlin.